WFPS-TME-060
SEPTEMBER 30, 1977

Conf-771029--197

IMPURITY AND GAS THROUGHPUT CONTROL FOR TNS

fusion power
systems department

Westinghouse Electric Corporation
P.O. Box 10864, Pgh. Pa. 15236

DISCLAIMER

WFPS-TME-060
SEPTEMBER 30, 1977

IMPURITY AND GAS THROUGHPUT CONTROL FOR TNS

E. W. SUCOV*

PREPRINT OF A PAPER TO BE PRESENTED AT THE
SEVENTH SYMPOSIUM ON ENGINEERING PROBLEMS OF FUSION RESEARCH,
KNOXVILLE, TENNESSEE, OCTOBER 25-28, 1977

*WESTINGHOUSE RESEARCH & DEVELOPMENT LAB

fusion power systems department

Westinghouse Electric Corporation
P.O. Box 10864, Pgh. Pa. 15236

ACKNOWLEDGEMENT

This work was performed for the Oak Ridge National Laboratory Fusion Energy Division, under U.S. Energy Research and Development Administration Contract W-7405-ENG-26, Subcontract 7117. Reproduction, translation, publication, use and disposal, in whole or in part, by or for the United States Government is permitted.

LEGAL NOTICE

FOREWORD

The Division of Magnetic Fusion Energy within the U.S. Energy Research and Development Administration has initiated within the fusion development program for tokamak power reactors a series of systems studies aimed at the definition of subsequent generations of tokamak devices leading to a commercial prototype reactor. Since April, 1976, a design team composed of representatives from the ORNL Fusion Energy Division and the Westinghouse Fusion Power Systems Department has been engaged in scoping studies associated with the definition of The Next Step (TNS) in the tokamak program after the TFTR. Provisional goals established for TNS include:

- achievement of ignition
- demonstration of burning dynamics
- evaluation of design requirements and solutions for long pulse operation
- features which extrapolate to a viable power reactor
- availability in the mid-to-late 1980's

It is in this context that the work reported herein was performed.

IMPURITY AND GAS THROUGHPUT CONTROL FOR TNS

SUMMARY

A model of the interaction between an ignited plasma and a wall is utilized to study the impact of impurities and recycled fuel ions and helium ash on the burn time of the plasma. The model indicates that the impurity concentration, n_{im}, grows exponentially toward a maximum value determined by the confinement time for impurities, τ_{im}, the sputtering coefficient, S_i, and the isolation coefficient, α. The time for n_{im} to reach a critical value and quench the plasma was determined for representative impurities, C, Mo, W, Fe, under various conditions of plasma temperature. Methods for extending the burn time by minimizing the effective sputtering coefficient of the wall and increasing the isolation of the plasma from the wall are reviewed. The carbides, B_4C and SiC, are found to have encouraging sputtering properties but their thermal, chemical and mechanical properties need to be evaluated before they can be recommended for use as first walls. The magnetic divertor is the preferred isolation scheme. Because the divertor carries impurities and leaked fuel and helium ions to a burial chamber, required pumping speeds are found to be very high for TNS plasmas and supplemental particle trapping systems must be introduced in order to reduce the required pump speed to attainable values.

MODEL FOR IMPURITY GENERATION AND CONTROL

A plasma-wall interaction model is depicted schematically in Figure 1. Charged (D^+, T^+, He^{++}, impurity) and neutral (D°, T°) particle fluxes emerge from the plasma and strike the wall, with the charged particle fluxes being reduced by a factor α_u due to particle removal (e.g., by a divertor). A fraction, R, of the remaining particles are reflected from the wall as low energy neutrals. The impinging particles also produce impurities at a rate determined by the sputtering coefficient, S. The returning neutral particles (D°, T°, He°, impurity) are reduced by a factor α_{sh} due to particle removal mechanisms such as density gradient reversal or a divertor and initiate a series of charge-exchange reactions leading to emergence of hot D° and T° from the plasma. This model has not included impurity desorption from the walls since this can, in principle, be reduced to very low levels by conditioning the walls.

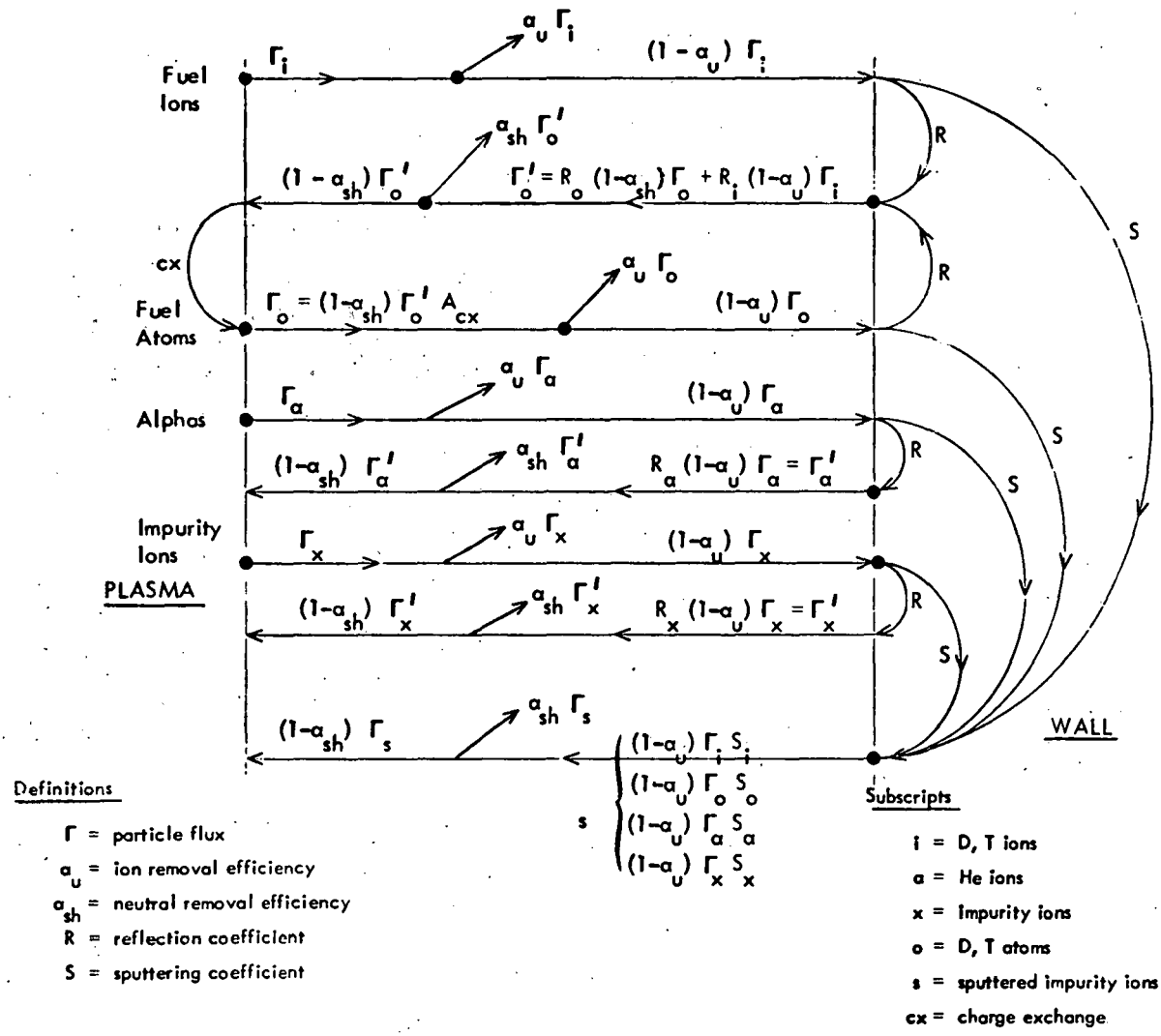

Figure 1. Plasma wall interaction model.

This complicated model can be much simplified by recognizing that $\Gamma_i >> \Gamma_x, \Gamma_\alpha, \Gamma_o$. Thus, charge exchange bombardment will be neglected and the dominant flux to the wall will be that due to the fuel ions. Figure 2 shows the simplified model.

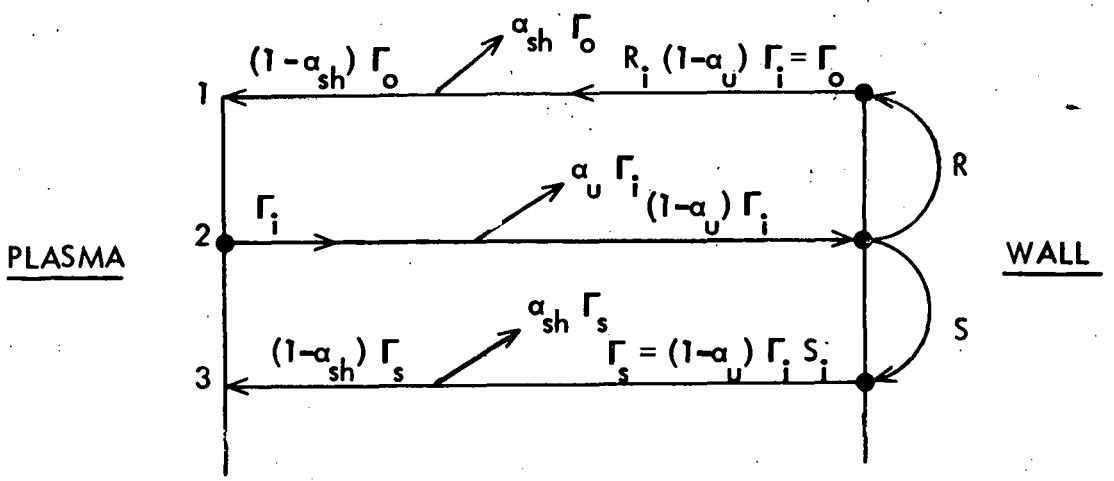

Figure 2. Simplified model of plasma wall interaction.

Line 1 describes the entrance of recycled fuel and helium atoms into the plasma at a rate

$$(1 - \alpha_{sh})\ \Gamma_o = (1 - \alpha_{sh})\ (1 - \alpha_u)\ \Gamma_i\ R_i \qquad (1)$$

and line 3 describes the entrance of sputtered impurities into the plasma at a rate

$$(1 - \alpha_{sh})\ \Gamma_s = (1 - \alpha_{sh})\ (1 - \alpha_u)\ \Gamma_i\ S_i \qquad (2)$$

IMPURITIES DECREASE BURN TIME

The effect of impurities (alphas and higher Z elements such as C, O, Fe, Mo, etc.) on the burn time of the plasma is felt in two ways. The first is through radiation losses from the plasma which compete with heating processes and can prevent the plasma from maintaining ignition temperature. For the TNS case, where neutral beam heating is expected to raise the plasma temperature to about 14 keV, bremsstrahlung radiation is the dominant radiative loss. The power lost this way is:

$$P_{br} = 5 \times 10^{-31} n_e^2 Z_{eff} T_e^{1/2} \quad (W/cm^3) \tag{3}$$

where

$$Z_{eff} = (n_h Z_h^2 + n_{im} Z_{im}^2)/n_e. \tag{4}$$

In these relations, n is the particle density, Z is the atomic number of the particle, T is the temperature, and the subscripts e, h, and im refer to electrons, hydrogenic (D and T) fuel ions, and to impurity ions respectively. In the steady state burn mode the total power radiated from the TNS plasma is $25 \times 10^6 Z_{eff}$ (W). Thus, it is essential to ensure that Z_{eff} does not rise substantially beyond the specified value of 1.14. The main effort of the review was to examine and evaluate the various schemes that have been proposed to keep Z_{eff} low and to recommend a preferred scheme.

The second effect of impurities on the plasma burn time derives from the requirements of charge neutrality, that is,

$$n_e = n_h Z_h + n_\alpha Z_\alpha + n_{im} Z_{im}. \tag{5}$$

Thus, the presence of alphas and impurities force n_h to be less than n_e and cause the fusion power density,

$$p_f = \frac{n_h^2}{4} \overline{\sigma v} \; U_f, \tag{6}$$

to decrease as the alpha and impurity concentrations grow in a constant pressure plasma. In this equation, $\overline{\sigma v}$ is the fusion reaction rate coefficient for D and T and U_f = 17.6 MeV. Even if the impurity concentration can be kept low by the schemes that will be examined later, the alpha population will grow at the rate

$$\frac{dn_\alpha}{dt} = n_h^2 \overline{\sigma v} - \frac{n_\alpha}{\tau_\alpha} + (1 - \alpha_u)(1 - \alpha_{sh}) \frac{n_\alpha}{\tau_\alpha} R_\alpha \tag{7}$$

where τ_α is the confinement time of the alphas. In the absence of a divertor and with the reflection coefficient for alphas approximately unity the last two terms cancel and n_α grows linearly with time (to a first approximation).

In fact, a proper time dependent description of the plasma requires, in addition to Equation (5), simultaneous solution of a set of coupled particle and energy balance equations:

$$\frac{dn_h}{dt} = (1 - \alpha_u)(1 - \alpha_{sh}) \frac{n_h}{\tau_h} R_h - n_h^2 \overline{\sigma v} - \frac{n_h}{\tau_h} \tag{8}$$

and

$$\frac{d\left(\frac{3}{2} n_h T\right)}{dt} = n_h^2 \overline{\sigma v} \; U_\alpha - \frac{\left(\frac{3}{2} n_h T\right)}{\tau_E} . \tag{9}$$

Equations (5) and (9) show that the effect of increasing n_α, which decreases n_h, is to cause the plasma temperature to decrease. To be specific, $\frac{dn_\alpha}{dt} = n_h^2 \overline{\sigma v} = 5.4 \times 10^{20}$/sec during the steady state burn phase. The total number of ions in

the plasma, $n_h V_p = 2 \times 10^{20} \times 250 = 5 \times 10^{22}$ at the start of the burn phase. Thus, if the linear approximation is applied, n_α grows at the rate of about 1% of n_h per second so n_h and T will decrease at that rate, limiting the burn phase to about 20 sec when T has dropped below 10 keV. A more exact solution is being developed.

For the higher Z impurities, the impurity concentration will grow at the rate

$$\frac{dn_{im}}{dt} = (1 - \alpha_{sh})(1 - \alpha_u)\frac{n_i S_i}{\tau_i} - \frac{n_{im}}{\tau_{im}} \qquad (10)$$

where τ_{im} is the impurity particle confinement time. The solution to this equation is:

$$n_{im} = \frac{n_i S_i}{\tau_i}(1 - \alpha_u)(1 - \alpha_{sh})\tau_{im}[1 - \exp(-t/\tau_{im})]. \qquad (11)$$

Neoclassical diffusion theory predicts that impurity ions will diffuse up the fuel ion density gradient and collect in the center of the plasma, i.e., $\tau_{im} >> \tau_i$. For this case, n_{im} increases exponentially during the burn pulse and reaches its maximum at the value $n_i S_i \frac{\tau_{im}}{\tau_i}(1 - \alpha_u)(1 - \alpha_{sh})$ when $t >> \tau_{im}$. Figure 3 shows the maximum allowed impurity concentration that will permit ignition to occur as a function of plasma temperature[1]. The time for n_{im} (from Equation 11) to exceed the values in Figure 3, for the case $\tau_{im} = 100\ \tau_i$, $T_e = 10$ keV, and impact energy T_s of protons on the wall = 1 keV, defines the burn time of the plasma and is shown in Figure 4 as a function of divertor efficiency. It is clear that burn times of > 10 seconds will require some kind of divertor action.

If heavy impurities did not collect inside the plasma but rather diffused as rapidly as do the fuel ions, that is, $\tau_{im} = \tau_i$, then n_{im} would rapidly reach its maximum value of $n_i S_i (1 - \alpha_u)(1 - \alpha_{sh})$. Because S_i, at impact energy of 1 keV, is very close to the critical maximum value of n_{im}/n_i, a small amount of isolation or a

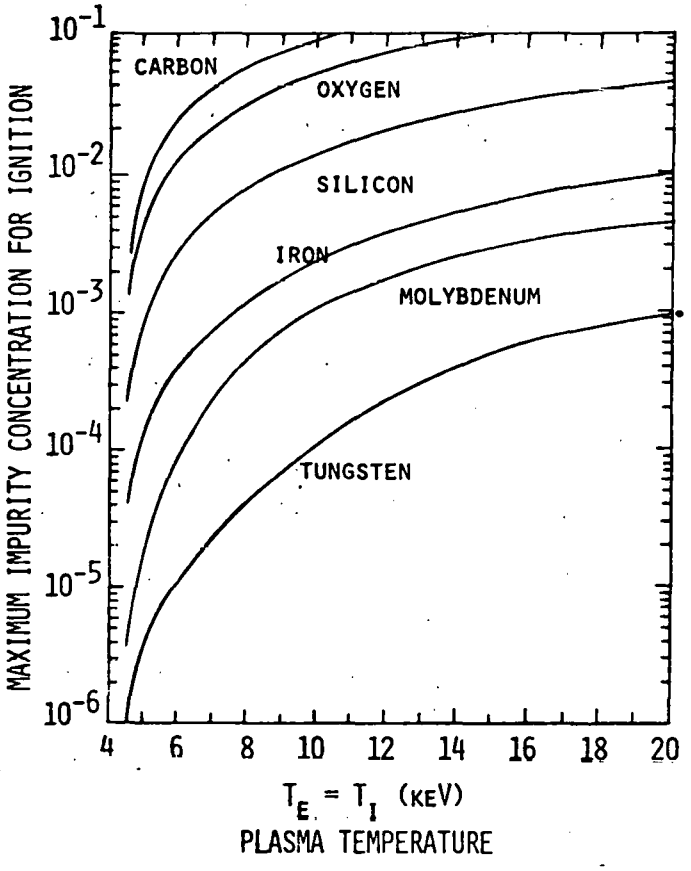

Figure 3. Maximum allowed impurity concentration for ignition as a function of plasma temperature, assuming zero nonradiative losses

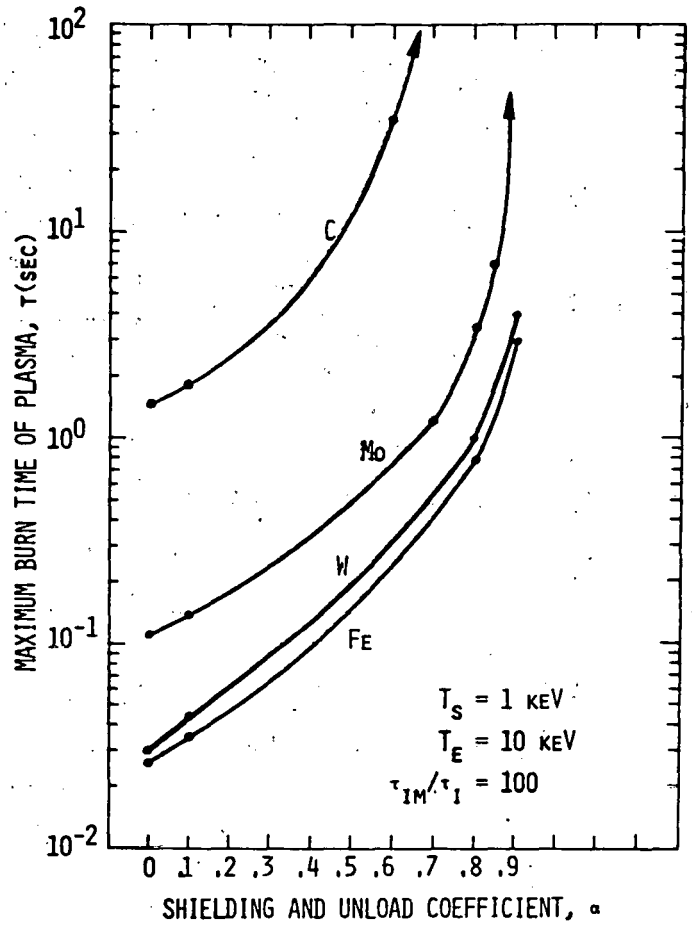

Figure 4. Maximum burn time of plasma with various impurities as a function of shielding and unload coefficient, α, for impact energy, T_S = 1 keV, plasma temperature, T_e = 10 keV, and confinement time of impurities, $\tau_{im} = 100\ \tau_i$.

slight decrease in the proton impact energy would bring S_i below these critical values. In that case, the burn times could be indefinitely long.

METHODS TO INCREASE PLASMA BURN TIME

Decrease Effect of Sputtering

The sputtering coefficient S_i varies with bombarding particle energy such that the peak of the curve is at about 1 keV for a variety of potential wall materials. This is shown in Figure 5. The peak value itself varies according to the material, and S_i decreases strongly as the incident energy decreases below 1 keV[2,3]. Since Z_{eff} varies as $n_{im} Z^2 \sim S_i Z^2$, Table 1 presents S_i for several candidate wall materials when bombarding energy is 1 keV as well as the "sputtering figure of merit" $S_i Z^2$. The larger values of $S_i Z^2$ indicate greater contributions to Z_{eff}; low values of $S_i Z^2$ are more desirable and therefore low Z materials offer one way to reduce the negative impact of impurities.

However, the option of decreasing the bombarding energy offers more spectacular improvement. This has led several authors[4,5] to propose a cold gas blanket to cool the emerging plasma ions to a temperature below the sputtering threshold. The cold gas blanket is an inherently unstable condition for the plasma-wall system and therefore must be maintained in dynamic equilibrium. However, the models used by these authors to calculate the various processes are simplified representations so it is not clear that equilibrium will be established over the appropriate range of energies, distances, and times. Whether these schemes will work can only be determined by experiment. It would be extremely important to test the cold gas blanket concept in currently available machines such as ISX or PLT.

Another approach to minimizing the effective sputtering coefficient would use a honeycomb wall[6] to capture the emitted particles. For cylindrical honeycomb cells of length, L, and diameter, D, a reduction in refluxing (of fuel ions) by a factor of 10 and a reduction in sputtering by a factor of four is calculated for L/D = 3. However, in the real situation within the vacuum chamber it is likely

that the sharp edges of the honeycomb will be eroded and that the trapping effectiveness of the surface will be rapidly reduced. In addition, the refluxing coefficient will approach unity as the honeycomb material saturates with fuel atoms. This approach seems to have limited utility.

The use of low Z materials for walls or liners of tokamak vacuum chambers, especially carbon (graphite) and carbides, has been investigated in some detail[7]. While physical sputtering yields for C, B_4C, and SiC are similar to those found for other candidate materials (see Table 1), the reactivity of high temperature carbon with hydrogen to form methane introduces an additional source of impurities into the plasma due to "chemical" sputtering. McCracken and co-workers have measured[8,9] methane formation from C, SiC, and B_4C and find peak emission at temperatures of 850, 800, and 500 K with chemical sputtering coefficients measured to be 4.5×10^{-2}; 1.3×10^{-2}; and 5.5×10^{-3}, respectively. When these higher values of S_i are used, the sputtering figures of merit, $S_i Z^2$, increase to 1.6, 0.47 and 0.2, respectively. Under these conditions materials such as Ti or Mo now have figures of merit comparable to that of C but the carbides are still superior to Ti and Mo. Further investigations of thermal, mechanical, chemical, fabrication and cost properties of the carbides appear to be warranted.

Prevent Impurity Atoms from Entering Plasma

Two major concepts have been proposed for preventing impurity atoms from entering the plasma: 1) magnetic divertor and 2) reversal of diffusion. The impurity atoms are assumed to have kinetic energy about 10 eV and to have a cosine law angular distribution.

When the removal scheme is a divertor, α_{sh} refers to the ability of the scrape-off layer to ionize the returning neutrals. The divertor field lines are assumed to capture all of the newly ionized particles as shown in Figure 6. The fraction of incoming neutrals that are ionized is given by:

$$\alpha_{sh} = 1 - \exp\left[-\frac{1}{v_x}\int_0^w \overline{\sigma_i v_e}\, n_s\, dx\right] \qquad (12)$$

TABLE 1

SPUTTERING FIGURE OF MERIT, $S_i Z^2$, FOR VARIOUS MATERIALS

WHEN BOMBARDING PROTONS ARE AT 1 keV ENERGY

Material	Z	Z^2	S_i	$S_i Z^2$
C	6	36	7×10^{-3}	0.25
B_4C	6	36	1.2×10^{-2}	0.43
SiC	6	36	7×10^{-3}	0.25
Ti	22	484	3×10^{-3}	1.46
SS	26(Fe)	676	10^{-2}	6.76
Nb	41	1680	3×10^{-3}	5.05
Mo	42	1750	10^{-3}	1.75
W	74	5500	6×10^{-4}	3.30

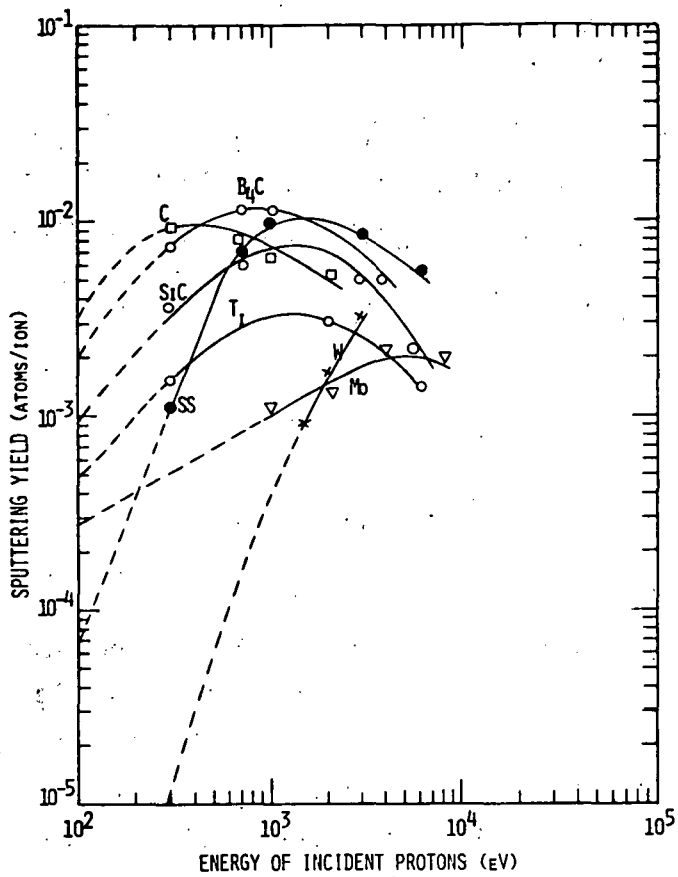

Figure 5. Physical sputtering yield is a function of impact energy and target material.

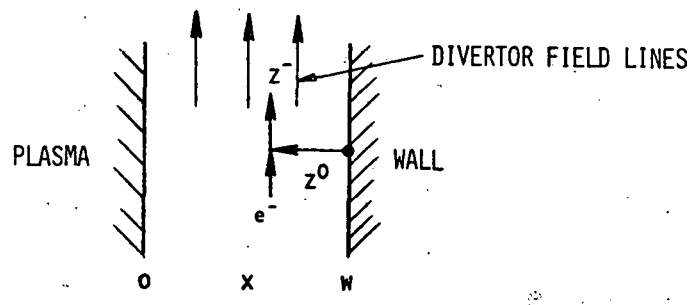

Figure 6. Schematic of divertor action showing neutral impurity atoms, Z°, becomong ionized by electron impact in the scrape-off layer of width, w, and being removed by the divertor field.

where v_x is the velocity of the impurity atoms, σ_i is the cross section for ionizing the impurity particles with electrons of velocity v_e and density n_s in the scrape-off layer of width w. Since $\overline{\sigma_i v_e}$ is essentially constant ($\sim 3 \times 10^{-7}$ cm^3 s^{-1}) when $v_e >> v_x$, it can be taken outside the integral and evaluated separately. Thus, in order for $\alpha_{sh} \geq 0.9$ for all impurities, the integral $\int ndx = nw$ must be $\geq 10^{13}$ cm^{-2}. The integral is evaluated approximately from the equilibrium relation

$$\int_o^w ndx = nw \approx n_p \, a_p \, \tau_s / \tau_p \qquad (13)$$

where n_p is the average plasma density, a_p is the plasma radius, τ_p is the ion confinement time ≈ 0.3 sec, and τ_s is the time for an ion to reach the burial chamber in one pass $= 2\pi R_o / v_x$. When values for TNS parameters are substituted in Equation (13), it is found that $nw \simeq 10^{14}$ cm^{-2}. Thus, $\alpha_{sh} = 0.9$ is a very conservative value for the shielding capability of a poloidal divertor on a TNS plasma. If a bundle divertor is considered, τ_s increases (because the divertor opening has a smaller probability of intersecting the ion flow) and therefore the shielding capability increases even more.

Another approach to increasing α_{sh} derives from neoclassical particle diffusion models which predict that the flux of impurities is controlled by the gradient of the hydrogen plasma and will diffuse toward the point of maximum hydrogen density. For tokamaks exhibiting the well-known parabolic density distribution, impurities will be captured in the central region of the plasma. However, if the profile of n(r) could be modified to exhibit a local peak near the outer edge of the plasma, impurities would be trapped there and be prevented from entering the hot core. An additional benefit of this mechanism results from the fact that the trapped impurities would radiate their energy to the wall and effectively cool the plasma edge, thereby decreasing the likelihood of sputtering. This scheme requires that a stable relatively dense and cold gas blanket exist between the plasma and the wall.

Brandt[10] and his group in the Netherlands have studied the dense gas blanket concept and find that, for steady state tokamaks, pressure equilibrium between the blanket and the hot plasma cannot be maintained. This is because inward diffusion of the neutral gas is not affected by the magnetic field while the ambipolar outward diffusion of the hot ions is restrained; this leads to a pressure buildup in the center.

Ohkawa[11] has calculated that impurity diffusion can be reversed by providing a source of protons (hydrogen gas) on one side of the plasma (e.g., the top of the torus) and a sink on the other (see Figure 7). In order to pump impurities out of the system, the ratio of particle injection to particle loss rates for the TNS must be 3.5. The particle loss rate from the TNS plasma is 16.8×10^{22} DT/s so the injection rate would have to be 55×10^{22}/s making a total gas load of 72×10^{22} particles/s $\approx 10^4$ torr liter/sec that the vacuum pumps must handle. Even if the exhaust pumps are required to maintain a pressure of only 10^{-3} torr, this would require a pumping speed of $\sim 10^7$ liter/sec; evacuating and processing this high gas flow represents a serious engineering problem.

While the neoclassical particle diffusion model has apparently been confirmed by Russian investigators[12] for the TM-3, reports from the TFR team[13,14] indicate that the light impurities (oxygen) stay in an outer shell, recycling with the wall, while the heavy impurities (Mo) are distributed throughout the inner region more broadly than predicted by neoclassical theory. Experiments on the ST[15] which followed radiation from excited states of injected Al atoms showed that the higher ionization states were indeed peaked closer to the center of the plasma as predicted by neoclassical diffusion theory. Hogan[16] suggests that higher current density plasmas might generate an MHD instability causing anomalous flow outward and that, in reactor grade tokamaks, the high Z impurities would peak at the outside of the plasma. The unsettled state of present understanding of impurity diffusion suggests that schemes depending on reversing the concentration gradient be considered with caution.

Prevent Emerging Ions from Striking the Wall

A magnetic divertor can capture and remove ions that leak from the plasma as shown in Figure 8; this is the unload function. The density of ions in the scrape-off layer is assumed to fall exponentially according to the relation

$$n(x) = n_s \exp(-x/\lambda) \tag{14}$$

where n_s is the density of ions at the separtrix, x is the distance into the scrape-off layer of width w, and $\lambda = \sqrt{D_\perp \tau_{||}}$ is the e-folding distance resulting from transport across the field lines with the diffusion coefficient $D_\perp$ subject to losses along the field lines with a residence time $\tau_{||}$. In order for $\alpha_u \geq 0.9$, w must be chosen such that $n(w) \leq 0.1\ n_s$; that is, $\exp(-w/\lambda) \leq 0.1$ and $w \geq 2.3\ \lambda$. The diffusion coefficient can be taken to be ~10% Bohm diffusion, that is $D_\perp \sim 10^4$ cm^2/sec, and $\tau_{||} \sim \tau_s = 2\pi R_o/v_H = 10^{-4}$ sec, so $\lambda \sim 1$ cm and $w \geq 2.3$ cm. This is the case for a free flowing ion stream. However, ions in the scrape-off layer of a D-shaped plasma experience a confining mirror field, since the toroidal field is greater at the divertor opening than at the plasma equator. This increases the residence time by a factor of about 50 since ions can only enter the opening by scattering into the mirror loss cone. For the mirror case, assuming $D_\perp$ stays the same, λ becomes ~7 cm and $w \geq 15$ cm.

The consequence of the mirror confined case on the shielding efficiency of the scrape-off layer is to require that $n_s \geq 10^{13}/w \geq 6 \times 10^{11}$ cm^{-3} which is easily achieved in a TNS plasma whose average density is 2×10^{14} cm^{-3}.

Handling the Gas Throughput when Divertors are Used

The gas removal system for the divertor must reduce the pressure in the burial chamber to about 10^{-6} torr. The model in Figure 2 indicates that the gas load into the burial chamber = $\Gamma_i (\alpha_u + R_i \alpha_{sh} (1 - \alpha_u) + S_i \alpha_{sh} (1 - \alpha_u)$ is essentially leaked fuel ions since $\alpha_u \approx 1$ and $R_i >> S_i$. For convenience it will be assumed that all the leakage flux, Γ_i = 2400 torr liter/s, is delivered to the

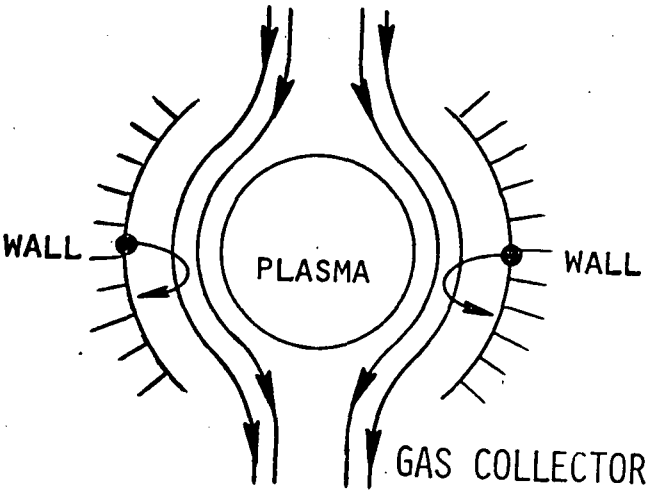

Figure 7. Schematic of concept of impurity diffusion reversal by gas flow showing gas source above plasma and gas collector below the plasma.

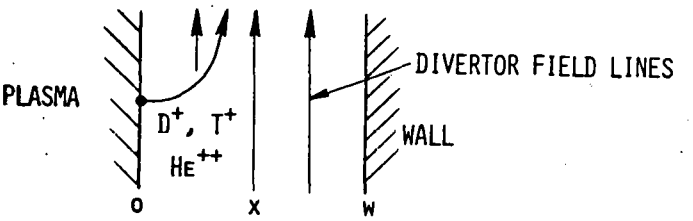

Figure 8. Schematic of unload divertor action showing plasma ions leaking from the plasma into the scrape-off layer and being removed by the divertor field.

burial chamber. To maintain $p = 10^{-6}$ torr will require a total pump speed $S = 2.4 \times 10^{9}$ liter/s. This could be generated by 24,000 m^2 of cryopanels, assuming 10 liter/s pumping speed per cm^2 of panel. Placing cryopanels in the burial chamber exposes them to severe heating from neutrons and radiation from nearby hot structure so there is strong incentive to investigate supplementary gettering systems to reduce the required pumping speed.

Gettering of hydrogenic ions in Mo, Ti, Ta, Nb, Zr, Li and an alloy of Zr/Al, takes place with an efficiency $s \geq 90\%$ over a limited temperature range[17] (see for example, Figure 9). However, the preferred getter material is Ti or Zr for the following reasons: $s = 0$ for Mo at doses $> 5 \times 10^{16}$ ions/cm^2 (30 sec dose will be 10^{19} ions/cm^2); liquid lithium is very difficult to pump against a magnetic field; Zr/Al surfaces are quickly contaminated by impurity atoms such as oxygen. Placing these getters in the divertor burial chamber will reduce the load on the vacuum pumps by a factor of 10, reducing the required pump speed to 2.4×10^{8} liter/sec; this is still a very high speed.

The sticking coefficient of the getters can be increased substantially by arranging them geometrically so that those particles which are not captured at the initial contact point are forced to contact additional surfaces. One concept which has been studied forms the getter surfaces into nested chevrons, as in Figure 10. In this arrangement the direction of the incident particles is well-defined since they travel along the divertor magnetic field lines. They enter the nested chevrons at a specific angle and suffer multiple bounces before a small fraction of the incident flux escapes as randomly moving particles into the vacuum pumping region. Analysis of this concept[18] showed that s_{eff} increased from 0.9 to at least 0.999 and that $S_{i_{eff}}$ decreased from 10^{-2} to 10^{-4} for reasonable spacing and dimension of the chevron. This reduces the required pumping speeds to $\sim 10^{6}$ liter/s which can be generated quite easily with about 10 m^2 of cryopanels.

Helium ions which will be generated at the rate of 5.4×10^{20}/sec, must also be pumped away. The above getters do not trap helium and cryosorption panels must be supercooled to below 4 K to capture helium. In addition, the cryopanels must be

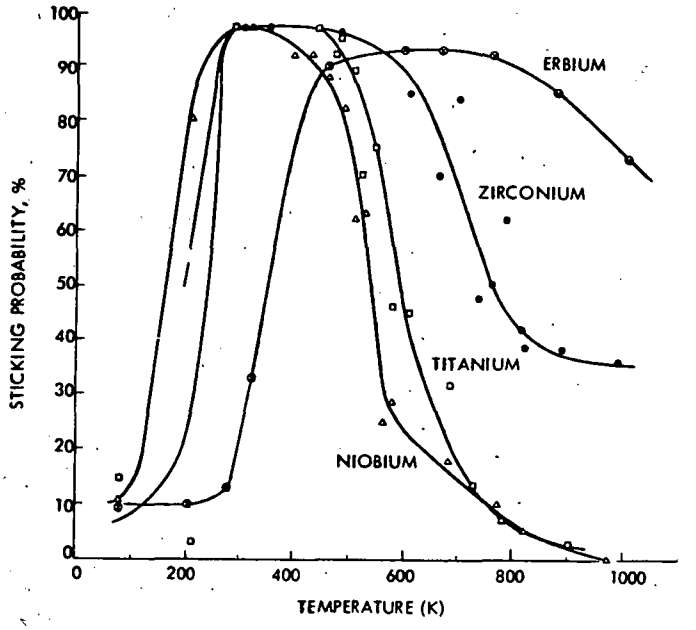

Figure 9. Temperature dependence of the sticking probabilities of D^+ ions in Niobium, Titanium, Zirconium, and Erbium. The maximum sticking probabilities are as high as 96%. Over a wide temperature range, the sticking probability is > 80%.

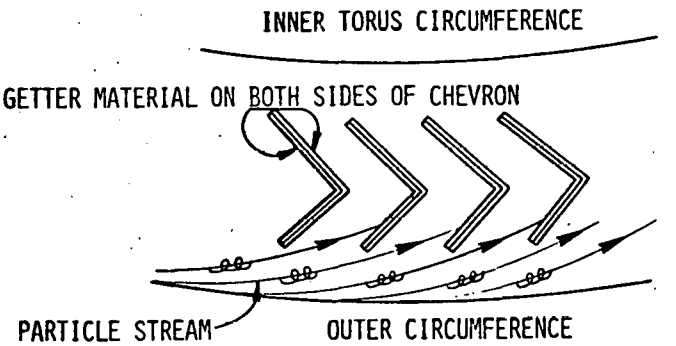

Figure 10. Chevron arrangements that intercept sputtered and re-emitted particles can increase trapping efficiency by a factor of 10^3.

multi staged both thermally and physically in order to pump both H and He. This problem may be solved by using a Nb getter. Figure 11 shows that Nb exhibits close to 100% trapping up to doses of 10^{17} ions/cm^2[19]. It could be fabricated into chevron shapes and interspersed among the Ti and/or Zr chevrons. The minimum area required to handle a thirty second pulse, before reaching the above saturation level, is 16 m^2.

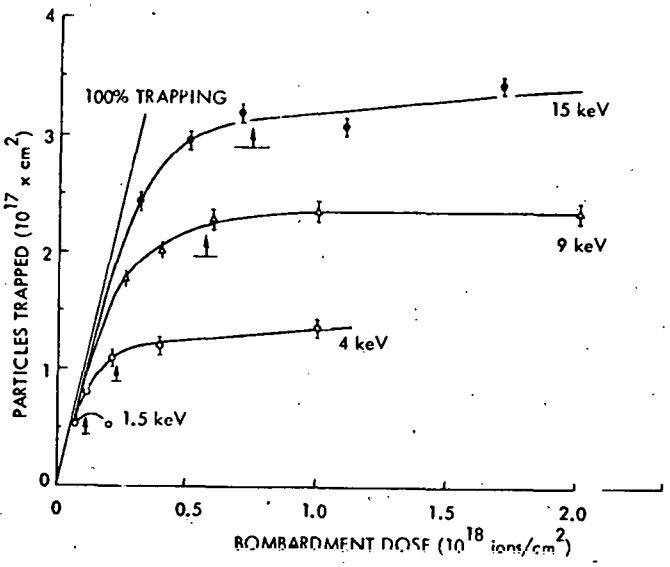

Figure 11. Saturation curves of the trapping of ^{3}He ions in a Niobium single crystal for different energies implanted to different doses in a random direction. The trapping efficiency is ∿ 100% at a dose of < 10^{17} cm^2 at 1.5 keV.

ACKNOWLEDGMENT

This work was performed for the Oak Ridge National Laboratory Fusion Energy Division under U.S. Energy Research and Development Administration Contract W-7405-ENG-26, Subcontract 7117.

REFERENCES

1. Jensen, R.V., et al, "Critical Impurity Concentrations for Power Multiplication in Beam Heated Toroidal Fusion Reactors," Princeton Plasma Physics Lab Report, PPPL-1350, April 1977
2. Scherzer, B.M.U., B. Behrisch, and J. Roth, "Wall Erosion by Physical and Chemical Sputtering and Blistering," International Symposium on Plasma-Wall Interactions, Julich, October 1976.
3. Cohen, S.A., "Sputtering Predictions for ST and PLT," Princeton Plasma Physics Lab Report, MATT 1171, Princeton, December 1975.
4. Hughes, M.N., "Numerical Calculations of Impurity Transport in JET," Workshop on the Present Status of JET, Garching, March 25-26, 1975.
5. Gibson, A., et al, "Impurity Control in Tokamaks," IAEA Second Large Tokamak Meeting, November 1976, Princeton, N. J.
6. Cramer, S.N., and E.M. Oblow, "Reduction of Re-fluxing Neutral Particles into a CTR Plasma by Use of a Honeycomb Wall," Nucl. Fus. 16, 158 (1976).
7. Rovner, L.H., R.F. Bourque, and K.Y. Chen, "Application of Low Atomic Number Ceramic Materials to Fusion Reactor First Walls," EPRI-ER-216, August 1976. (Availability: Electric Power Research Institute, Palo Alto, CA)
8. Erents, S.K., C.M. Braganza, and G.M. McCracken, "Methane Formation During Interaction of Energetic Protons and Deuterons with Carbon," Conference on Surface Effects in Controlled Fusion Devices, San Francisco, February 1976.
9. Braganza, C., G.M. McCracken, and S.K. Erents, "Methane Formation During Hydrogen Ion Irradiation of Silicon and Boron Carbide," International Symp. on Plasma Wall Interaction, Julich, Germany, October 1976.
10. Brandt, B. and C.M. Broams, "Gas Blanket Concept," in "Fusion Reactor Design Problems," pp 385-392, IAEA, Vienna, Austria, 1974.
11. Ohkawa, T., Kakuyugo-Kenkyu 32, 67 (1974).
12. Gervids, V.I., and V.A. Krupin, "Investigation of Impurity Diffusion in a Tokamak by Special Methods," JETP Lett, 18, No. 2, 60 (1973).
13. Equipe TFR, "Line Radiation in the Visible and in the Ultraviolet in TFR Tokamak Plasmas," Nucl. Fus. 15, 1053 (1975).
14. "Report on the Seventh European Conference on Controlled Nuclear Fusion," Lausanne, Switzerland, September, 1975, Nucl. Fus. 16, 169 (1976).
15. Meservey, E.B., et al, "Aluminum Limiter Experiment in ST Tokamak," Nucl. Fus. 16, 593 (1976).
16. Hogan, J., ERDA Meeting on Status of Impurities in Tokamaks, Unpublished Data, May 1976.
17. McCracken, G.M., and J.H.C. Maple, "Trapping of Hydrogen Ions in Mo, Ti, Ta, and Zr," Brit. J. Appl. Phys. 18, 919 (1967).
18. Sucov, E.W., D.K. McLain, and J.W.H. Chi, "Efficient Particle Removal from Tokamak Fusion Reactors," Trans. ANS Meeting, Vol. 24, November 1976, pg. 59.
19. Behrisch, R., et al, "Trapping of Low Energy Helium Ions in Niobium," Jnl. Nucl. Materials 56, 365 (1975).

INTERNAL DISTRIBUTION

1. Author
2. J. H. Fink
3. C. A. Flanagan
4. J. W. French
5. G. Gibson
6. D. J. Grove
7. G. W. Hardigg
8. F. M. Heck
9. J. L. Johnson
10. A. R. Jones
11. C. K. Jones
12. J. S. Karbowski
13. D. Klein
14. W. P. Kovacik
15. G. A. Krist
16. I. Liberman
17. C. J. Mole
18. R. P. Rose
19. Z. M. Shapiro
20. R. A. Smith
21. C. C. Sterrett
22. R. W. Stooksberry
23. T. C. Varljen
24. R. W. Warren
25. P. N. Wolfe
26. M. K. Wright
27. J. L. Young

28-41. Fusion Library

42-43. ARD Library

OAK RIDGE NATIONAL LABORATORY DISTRIBUTION

44. J. K. Ballou
45. J. F. Clarke
46. P. N. Haubenreich
47. M. S. Lubell
48. O. B. Morgan

49-63. M. Roberts

64. M. W. Rosenthal
65. T. E. Shannon
66. D. Steiner
67. W. C. Stoddart
68. D. W. Swain

EXTERNAL DISTRIBUTION

1. J. L. Anderson, Los Alamos Scientific Laboratory, P. O. Box 1663, Los Alamos, NM 87545.
2. D. J. Anthony, General Electric Co., Schenectady, NY 12345.
3. C. C. Baker, General Atomic Co., San Diego, CA 92138.
4. A. A. Bishop, Nuclear Engineering Programs Director, Chemical Engineering Department, University of Pittsburgh, Pittsburgh, PA 15261.
5. S. L. Bogart, Energy Research and Development Administration, Division of Magnetic Fusion Energy, Mail Stop G-234, Washington, DC 20545.
6. S. J. Buchsbaum, Bell Laboratories, Crawford Corner Road, Holmdel, NJ 07733.
7. R. W. Bussard, Energy Resources Group, Inc., 1500 Wilson Blvd., Suite 505, Arlington, VA 22209.
8. Yung-An Chao, Nuclear Science and Engineering Div., Carnegie-Mellon University, Schenley Park, Pittsburgh, PA 15213.
9. R. N. Cherdack, Burns & Roe, Inc., 283 Highway 17, Paramus, NJ 07652.
10. F. E. Coffman, Energy Research and Development Administration, Division of Magnetic Fusion Energy, Mail Stop G-234, Washington, DC 20545.
11. D. R. Cohn, Francis Bitter Laboratory, MIT, 120 Albany St., Cambridge MA 02139.
12. R. W. Conn, Nuclear Engineering Dept., University of Wisconsin, Madison, WI 53706.
13. E. C. Creutz, National Science Foundation, 1800 G Street, N.W., Washington, DC 20440.

14. H. S. Cullingford, Energy Research and Development Administration, Division of Magnetic Fusion Energy, Mail Stop G-234, Washington, DC 20545.
15. R. C. Davidson, U.S. Energy Research and Development Administration, Division of Magnetic Fusion Energy, Mail Stop G-234, Washington, DC 20545.
16. N. A. Davies, Energy Research and Development Administration, Division of Magnetic Fusion Energy, Mail Stop G-234, Washington, DC 20545.
17. S. O. Dean, Energy Research and Development Administration, Division of Magnetic Fusion Energy, Mail Stop G-234, Washington, DC 20545.
18. A. Favale, Grumman Aerospace Corp., Bethpage, NY 11714.
19. S. Fernback, Lawrence Livermore Laboratory, Livermore, CA 94551.
20. E. von Fischer, Bechtel Corp., P. O. Box 3965, San Francisco, CA 94119.
21. H. K. Forsen, Exxon Nuclear Co., 777 106th Ave. N.E., Bellevue, WA 98004.
22. T. K. Fowler, University of California, Lawrence Radiation Laboratory, P. O. Box 808, Livermore, CA 94551.
23. H. P. Furth, Princeton Plasma Physics Laboratory, Princeton University, P. O. Box 451, Princeton, NJ 08540.
24. M. B. Gottlieb, Princeton Plasma Physics Laboratory, Princeton University, P. O. Box 451, Princeton, NJ 08540.
25. W. C. Gough, Electric Power Research Institute, Palo Alto, CA 94304.
26. J. Nelson Grace, Energy Research and Development Administration, Division of Magnetic Fusion Energy, Mail Stop G-234, Washington, DC 20545.
27. R. Harder, General Atomic Co., P. O. Box 81608, San Diego, CA 92138.
28. C. D. Henning, Energy Research and Development Administration, Division of Magnetic Fusion Energy, Mail Stop G-234, Washington, DC 20545.
29. G. K. Hess, Jr., Division of Magnetic Fusion Energy, U.S. Energy Research and Development Administration, Washington, DC 20545.
30. A. G. Hill, Plasma Fusion Center, Room 4-232, Massachusetts Institute of Technology, 77 Massachusetts Avenue, Cambridge, MA 20139.
31. R. L. Hirsch, Exxon Nuclear Corp., RM. 4330, 1251 Avenue of the Americas, New York, NY 10020.
32. T. Kammash, The University of Michigan, College of Engineering, Dept. of Nuclear Engineering, Ann Arbor, MI 48109.
33. E. E. Kintner, Energy Research and Development Administration, Division of Magnetic Fusion Energy, Mail Stop G-234, Washington, DC 20545.
34. G. Kulcinski, Nuclear Engineering Dept., University of Wisconsin, Madison WI 53706.
35. D. Kummer, McDonnell Douglas, P. O. Box 516, St. Louis, MO 63166.
36. V. A. Maroni, Argonne National Laboratory, 9700 S. Cass Ave., Argonne, IL 60439.
37. D. M. Meade, Princeton Plasma Physics Laboratory, Princeton University, P. O. Box 451, Princeton, NJ 08540.
38. G. H. Miley, Nuclear Engineering Program, 214 Nuclear Engineering Laboratory, University of Illinois, Urbana, IL 61801.
39. R. Mills, Princeton Plasma Physics Laboratory, Princeton University, P. O. Box 451, Princeton, NJ 08540.
40. K. Moses, Energy Research and Development Administration, Division of Magnetic Fusion Energy, Mail Stop G-234, Washington,DC 20545.
41. M. R. Murphy, Energy Research and Development Administration, Division of Magnetic Fusion Energy, Mail Stop G-234, Washington, DC 20545.
42. S. Naymark, Nuclear Services Corp., 1700 Dell Ave., Campbell, CA 95008.
43. J. O. Neff, Energy Research and Development Administration, Division of Magnetic Fusion Energy, Mail Stop G-234, Washington, DC 20545.
44. T. Ohkawa, General Atomic Co., P. O. Box 608, San Diego, CA 92112.
45. J. Powell, Brookhaven National Laboratory, Upton, Long Island, NY 11973.
46. J. R. Purcell, General Atomic Co., P. O. Box 608, San Diego, CA 92112.

47. P. J. Reardon, Princeton Plasma Physics Laboratory, Princeton University, P. O. Box 451, Princeton, NJ 08540.
48. D. J. Rose, Department of Nuclear Engineering, Massachusetts Institute of Technology, Cambridge, MA 02139.
49. P. Sager, General Atomic Co., P. O. Box 608, San Diego, CA 92112.
50. G. A. Sawyer, Los Alamos Scientific Laboratory, P. O. Box 1663, Los Alamos, NM 87545.
51. L. C. Schmid, Pacific Northwest Laboratories, Battelle Blvd., P. O. Box 999, Richland, WA 99352.
52. M. A. Schultz, Nuclear Engineering Department, The Pennsylvania State University, 231 Sackett Building, University Park, PA 16802.
53. Weston M. Stacey, Jr., Georgia Institute of Technology, Atlanta, GA 30332.
54. C. M. Stickley, Division of Laser Fusion, U.S. Energy Research and Development Administration, Washington, DC 20545.
55. C. E. Taylor, Lawrence Livermore Laboratory, Mail Code L-384, P. O. Box 808, Livermore, CA 94550.
56. V. Teofilo, Pacific Northwest Laboratories, Battelle Blvd., P. O. Box 999, Richland, WA 99352.
57. K. Thomassen, Lawrence Livermore Laboratory, P. O. Box 808, Livermore, CA 94550.
58. B. Twining, Energy Research and Development Administration, Division of Magnetic Fusion Energy, Mail Stop G-234, Washington, DC 20545.
59. A. W. Trivelpiece, Engineering and Research, Maxwell Laboratories, Inc., 9244 Balboa Avenue, San Diego, CA 92123.
60. J. M. Williams, Energy Research and Development Administration, Division of Magnetic Fusion Energy, Mail Stop G-234, Washington, DC 20545.
61. H. H. Woodson, Department of Electrical Engineering, Universitv of Texas, Austin, TX 78712.
62. H. Yoshikawa, Westinghouse Hanford Co., P. O. Box 1970, Richland, WA 99352.
63. K. Zwilski, Energy Research and Development Administration, Division of Magnetic Fusion Energy, Mail Stop G-234, Washington, DC 20545.
64. Energy Research and Development Administration, Technical Information Center, P. O. Box 62, Oak Ridge, Tennessee 37830.